Journal of Visualized Experiments

Fabrication of Nanoheight Channels Incorporating Surface Acoustic Wave Actuation via Lithium Niobate for Acoustic Nanofluidics

--Manuscript Draft--

Article Type:	Invited Methods Article - JoVE Produced Video
Manuscript Number:	JoVE60648R3
Full Title:	Fabrication of Nanoheight Channels Incorporating Surface Acoustic Wave Actuation via Lithium Niobate for Acoustic Nanofluidics
Section/Category:	JoVE Engineering
Keywords:	Acoustofluidics; Nanofluidics; Nanofabrication; Surface Acoustic Waves; Room-Temperature Bonding; Lithium Niobate; Plasma Activated Bonding
Corresponding Author:	James Friend University of California-San Diego La Jolla, California UNITED STATES
Corresponding Author's Institution:	University of California-San Diego
Corresponding Author E-Mail:	jfriend@eng.ucsd.edu
Order of Authors:	Naiqing Zhang
	James Friend
Additional Information:	
Question	**Response**
Please indicate whether this article will be Standard Access or Open Access.	Standard Access (US$2,400)
Please indicate the **city, state/province, and country** where this article will be **filmed**. Please do not use abbreviations.	La Jolla, California, United States of America

TITLE:

Fabrication of Nanoheight Channels Incorporating Surface Acoustic Wave Actuation via Lithium Niobate for Acoustic Nanofluidics

AUTHORS AND AFFILIATIONS:

Naiqing Zhang[1], James Friend[1]

[1]Medically Advanced Devices Laboratory, Center for Medical Devices, Department of Mechanical and Aerospace Engineering, Jacobs School of Engineering, and the Department of Surgery, School of Medicine, University of California San Diego, La Jolla, CA, USA

Corresponding author:
James Friend (jfriend@eng.ucsd.edu)

KEYWORDS:

acoustofluidics, nanofluidics, nanofabrication, surface acoustic waves, room-temperature bonding, lithium niobate, plasma activated bonding

SUMMARY:

We demonstrate fabrication of nanoheight channels with the integration of surface acoustic wave actuation devices upon lithium niobate for acoustic nanofluidics via liftoff photolithography, nano-depth reactive ion etching, and room-temperature plasma surface-activated multilayer bonding of single-crystal lithium niobate, a process similarly useful for bonding lithium niobate to oxides.

ABSTRACT:

Controlled nanoscale manipulation of fluids is known to be exceptionally difficult due to the dominance of surface and viscous forces. Megahertz-order surface acoustic wave (SAW) devices generate tremendous acceleration on their surface, up to 10^8 m/s^2, in turn responsible for many of the observed effects that have come to define acoustofluidics: acoustic streaming and acoustic radiation forces. These effects have been used for particle, cell, and fluid manipulation at the microscale, although more recently SAW has been used to produce similar phenomena at the nanoscale through an entirely different set of mechanisms. Controllable nanoscale fluid manipulation offers a broad range of opportunities in ultrafast fluid pumping and biomacromolecule dynamics useful for physical and biological applications. Here, we demonstrate nanoscale-height channel fabrication via room-temperature lithium niobate (LN) bonding integrated with a SAW device. We describe the entire experimental process including nano-height channel fabrication via dry etching, plasma-activated bonding on lithium niobate, the appropriate optical setup for subsequent imaging, and SAW actuation. We show representative results for fluid capillary filling and fluid draining in a nanoscale channel induced by SAW. This procedure offers a practical protocol for nanoscale channel fabrication and integration with SAW devices useful to build upon for future nanofluidics applications.

INTRODUCTION:

Controllable nanoscale fluid transport in nanochannels—*nanofluidics*[1]—occurs on the same

length scales as most biological macromolecules, and is promising for biological analysis and sensing, medical diagnosis, and material processing. Various designs and simulations have been developed in nanofluidics to manipulate fluids and particle suspensions based on temperature gradients[2], Coulomb dragging[3], surface waves[4], static electric fields[5-7], and thermophoresis[8] over the last fifteen years. Recently, SAW has been shown[9] to produce nanoscale fluid pumping and draining with sufficient acoustic pressure to overcome the dominance of surface and viscous forces that otherwise prevent effective fluid transport in nanochannels. The key benefit of acoustic streaming is its ability to drive useful flow in nanostructures without concern over the details of the chemistry of the fluid or particle suspension, making devices that utilize this technique immediately useful in biological analysis, sensing, and other physicochemical applications.

Fabrication of SAW-integrated nanofluidic devices requires fabrication of the electrodes—the *interdigital transducer* (IDT)—on a piezoelectric substrate, lithium niobate[10], to facilitate generating the SAW. Reactive ion etching (RIE) is used to form a nanoscale depression in a separate LN piece, and LN-LN bonding of the two pieces produces a useful nanochannel. The fabrication process for SAW devices has been presented in many publications, whether using normal or lift-off ultraviolet photolithography alongside metal sputter or evaporation deposition[11]. For the LN RIE process to etch a channel in a specific shape, the effects on the etch rate and the channel's final surface roughness from choosing different LN orientations, mask materials, gas flow, and plasma power have been investigated[12-16]. Plasma surface activation has been used to significantly increase surface energy and hence improve the strength of bonding in oxides such as LN[17-20]. It is likewise possible to heterogeneously bond LN with other oxides, such as SiO_2 (glass) via a two-step plasma activated bonding method[21]. Room-temperature LN-LN bonding, in particular, has been investigated using different cleaning and surface activation treatments[22].

Here, we describe in detail the process to fabricate 40 MHz SAW-integrated 100-nm height nanochannels, often called *nanoslit* channels (**Figure 1A**). Effective fluid capillary filling and fluid draining by SAW actuation demonstrates the validity of both nanoslit fabrication and SAW performance in such a nanoscale channel. Our approach offers a nano-acoustofluidic system enabling investigation of a variety of physical problems and biological applications.

PROTOCOL:

1. Nano-height channel mask preparation

1.1. Photolithography: With a pattern describing the desired shape of the nanoheight channels (**Figure 1B**), use normal photolithography and lift-off procedures to produce nanoheight depressions in an LN wafer. These depressions will become nanoheight channels upon wafer bonding in a later step.

NOTE: The lateral dimensions of the nanoscale depressions are microscale in this protocol. Electron beam or He/Ne ion beam lithography can be used to fabricate channels with nanoscale

lateral dimensions; Ga^+-based ion beam lithography causes swelling and uneven substrate profiles[23]. The orientation of the two LN wafers should match, otherwise, thermal stress may cause the wafers or the bond between them to fail.

1.2. Sputter deposition to protect regions from dry etching: Place the wafer into the sputter deposition system. Draw down the chamber vacuum to 5×10^{-6} mTorr, allow Ar to flow at 2.5 mTorr, and sputter Cr at 200 W to produce a 400-nm thick sacrificial mask where reactive ion etching will be prevented when used in step 3 below.

1.3. Lift-off: Transfer the wafer into a beaker with sufficient acetone to completely immerse the wafer. Sonicate at medium intensity for 10 min. Rinse with DI water and dry the wafer with dry N_2 flow.

1.4. Dicing: Use a dicing saw to dice the entire wafer into individual chips with (typically) one nanoslit pattern per chip.

NOTE: The protocol can be paused here.

2. Nano-height channel fabrication

2.1. Reactive ion etching (RIE): Use RIE to etch nanoscale depressions into the uncovered regions of the LN substrate. Regions left covered by sacrificial Cr will be protected from etching. Set the RIE power to 200W, heat the chamber to 50 °C, draw down the chamber vacuum to 20 mTorr, set the SF_6 flow rate to 10 sccm, and etch for 20 min to produce a 120-nm deep nanoslit in LN.

2.2. Hole drilling for channel inlets and outlets: With double-sided tape, attach an etched LN chip to a small steel plate and the plate to the bottom of a petri dish. The Petri dish should be large enough to permit complete immersion of the LN chip and steel plate. Fill the Petri dish with water to fully immerse the chip. Attach a 0.5-mm diameter diamond drill bit to a drill press, and drill at a high speed of at least 10,000 rpm to machine the desired inlets and outlets. Drilling through a 0.5 mm thick substrate should take about 10 to 15 s[24] (**Figure 1B**).

NOTE: Immersion while drilling prevents excessive local heating and particulate jamming at the drill site. Other types of drill bits are unlikely to work, and hand drilling is not possible at any speed to our knowledge. Drill bit rotation speeds of 10,000 rpm or greater are recommended to avoid shattering the LN.

2.3. Cr wet etching: Use a diamond tip engraving pen to clearly mark the flat, unetched face of the drilled LN to keep track of which side the nanoheight channel is located in the remaining steps. Sonicate the chips in Cr etchant.

NOTE: The protocol can be paused here. It is exceedingly difficult to determine which side of the LN chip has the etched nanoscale depression after the Cr is removed. The sonication time

depends upon the etching rate and the Cr mask thickness.

3. Room-temperature Plasma Activated Bonding

3.1. Solvent cleaning LN chips: Collect chip pairs—one SAW device (fabricated by normal photolithography, sputter deposition, and lift-off procedures) and one etched nanoscale depression chip—together to prepare them for bonding. Immerse the chip pairs in a beaker of acetone placed in a sonication bath and sonicate for 2 min. Transfer the chips to methanol and sonicate for 1 min. Transfer the chips to DI water.

3.2. Piranha cleaning: Prepare piranha acid in a glass beaker in a well-ventilated hood, dedicated to the use of acid, by adding H_2O_2 (30% in water) to H_2SO_4 (96%) at a ratio of 1:3. Place all chips in a Teflon holder. Place the holder in the beaker and immerse all chips into the piranha solution for 10 min, then rinse the chips and holder sequentially in two separate DI water baths. Dry the chips with dry N_2 and immediately transfer them into oxygen (O_2) plasma activation equipment, keeping them covered during handling to avoid contamination.

CAUTION: Piranha solutions are highly corrosive, are strongly oxidizing, and are dangerous. Follow the specific rules handling them at your institution, but at least take extreme care and wear the proper safety equipment. Upon completion of the work, the piranha solution must be cooled for at least one hour before pouring into a dedicated waste container.

NOTE: It is necessary to rinse the LN chips twice in two DI water baths. Rinsing them once leaves residue behind that will likely ruin the bonding. Gold electrodes are used for IDTs because of their good resistance to piranha solution.

3.3. Plasma surface activation: Activate the chip surfaces using plasma with 120 W of power while exposed to O_2 flow at 120 sccm for 150 s. Immediately transfer the samples to a fresh DI water bath for at least 2 min.

NOTE: Plasma surface treatment quickly followed by DI water immersion will form hydroxyl groups upon the LN surface, increasing its free surface energy to later promote bonding.

3.4. Room-temperature bonding: Dry the samples with dry N_2 flow and carefully lay the nanoslit chip onto the SAW device chip in the desired position. Realign to produce the desired orientation. Then use tweezers or similar to push down upon the sample from its center to initiate the bond. Gently push down in areas that failed to bond after the initial push.

NOTE: The bonding may be easily seen through the transparent LN. Bonded regions are entirely transparent. LN that is not double-side polished will be more difficult to assess.

3.5. Heating after bonding: Place bonded samples in a sprung clamp to safely exert loads on it despite thermal expansion, and place the clamped samples into an oven at room temperature (25 °C). Set the oven heating temperature to 300 °C, ramp rate to 2 °C/min maximum, dwell time

to 2 h, and then to automatically shut off to allow it and the clamped samples within to naturally cool to room temperature.

NOTE: The protocol can be paused here. The bonding between hydroxyl groups produces water at the bond, and heating removes the water to drastically increase the bond strength. Modest clamping forces are sufficient. Attempting to bond two chips of different orientations or materials may cause cracks due to mismatched thermal expansion and consequent stress.

4. Experimental setup and testing

4.1. Observation: Observe the nanoslit under an inverted microscope. Include and rotate a linear polarizing filter in the optical path to suitably block birefringence-based image doubling in the LN. Use ultrapure DI water via the inlet to observe fluid motion in the completed nanoslit.

NOTE: Ultrapure liquid is strongly recommended to prevent clogging, especially after evaporation.

4.2. SAW actuation: Attach absorbers at the ends of the SAW device to prevent reflected acoustic waves. Use a signal generator to apply a sinusoidal electric field to the IDT at its resonance frequency of around 40 MHz. Use an amplifier to amplify the signal. Use an oscilloscope to measure the actual voltage, current, and power applied to the device. Record the fluid motion during SAW actuation within the nanoslit using a camera attached to the microscope.

REPRESENTATIVE RESULTS:

We perform fluid capillary filing and SAW-induced fluid draining in nano-height LN slits after successful fabrication and bonding of SAW integrated nanofluidic devices. Surface acoustic waves are generated by IDTs actuated by an amplified sinusoidal signal at the IDTs' resonance frequency of 40 MHz, and the SAW propagates into the nanoslit via a piezoelectric LN substrate. The behavior of the fluid in the nanoslit interacting with SAW may be observed using an inverted microscope.

We demonstrate fluid capillary filling in 100-nm tall channels of different widths. **Figure 2** shows capillary filling of ultrapure DI water into two 100-nm tall channels, one 400 µm wide and the other 40 µm wide. The drop of ultrapure water is delivered into the nanoslit through the inlet. Capillary forces drive fluid filling of the entire nanoslit, and the filling occurs more quickly with the narrower channel due to its larger capillary force. Capillary force-driven fluid filling using other fluids of different viscosities and surface tensions could be used, as could nanoslits of other heights to produce different results.

We also demonstrate SAW-induced fluid draining in a nanochannel by overcoming capillary pressure. Water in a 100-nm height slit has been drained to show a water-air interface with the maximum length at the middle (**Figure 3**), indicating maximum acoustic energy at middle of the SAW device. With strong acoustic pressure generated in the nanoslit, it also indicates good bonding strength using our plasma-surface-activated room-temperature LN bonding method. A threshold applied power of around 1 W is required to force the acoustic pressure to be larger

than the capillary pressure and drive a visible draining phenomenon (**Figure 4**). The maximum length of the air cavity which represents fluid surface energy shows a linear relationship with the applied acoustic power. It offers an effective tool for fluid actuation and potentially macro-biomolecule manipulation at the nanoscale. The effect of draining various fluids using SAW with different channel heights and widths could be further investigated.

FIGURE AND TABLE LEGENDS:

Figure 1: Images of fabricated devices. (**A**) Left: Gold electroded IDTs with a 0.7 mm aperture on LN substrate for 40 MHz SAW generation and propagation. Middle & Right: Bonded LN nanoslit device integrated with SAW for fluid actuation. A one-penny coin is shown as a scale reference at bottom. (**B**) Various reactive-ion-etched nano-height channel LN chips are shown with chromium sacrificial mask structures and after drilling 500-µm diameter holes for fluid inlets and outlets. Scale bar: 5 mm.

Figure 2: Fluid capillary filling in 100 nm-height channels. (**A1-A4**) Ultrapure water is drawn into a 400-µm wide nanoslit via capillary force over time, shown at the start (0 s) and 1, 2, and 4 s later, respectively. Small water drops can be seen at the top of the superstrate. (**B1-B4**) Ultrapure water is drawn into a 40 µm wide nanoslit via capillary force over time, shown at the start (0 s) and 0.1, 0.3, and 1 s later, respectively, indicating more rapid filling due to greater capillary force on a smaller amount of fluid. The small depressions at the top of the superstrate are evidence of hitting the surface with tweezers. Scale bar: 400 µm.

Figure 3: SAW-induced fluid draining in 1 mm-width 100 nm-height nanoslit. (**A-C**) A water-filled nanoslit is drained by 40 MHz SAW at an applied power of 1.31 W, 2.04 W, and 2.82 W, respectively. The SAW is propagating from top to bottom in the images. The interfacial line between the bonded and nanoslit regions is visible: note the color change. Scale bar: 200 µm.

Figure 4: SAW-induced air cavity length with respect to SAW applied power. The dewetting cavity length is approximately linearly dependent upon the applied power. The applied power should offer an acoustic pressure greater than the capillary pressure in the nanoslit, causing fluid drainage. The threshold applied power at which drainage appears is around 1 W in this case.

DISCUSSION:

Room-temperature bonding is key to fabricating SAW-integrated nanoslit devices. Five aspects need to be considered to ensure successful bonding and sufficient bonding strength.

Time and power for plasma surface activation

Increasing the plasma power will help increase the surface energy and accordingly increase the bonding strength. But the downside of increasing the power during plasma surface activation is the increase in surface roughness, which may adversely affect the nanoslit fabrication and fluid transport performance. It has been shown that the plasma surface activation time will not help increase the surface energy after a certain amount of time[21]. Thus, the plasma activation time and power need to be defined to maximize the surface energy but not at the expense of increased surface roughness.

Cleaning chips before bonding

Since there is only a nanoscale height channel after bonding, any micro-size particle will be an enormous obstacle and cause bonding failure. Piranha cleaning is used to remove all organic debris on the chip surfaces. After cleaning, it is strongly recommended to use a clean container to cover the chips and prevent contamination.

Orientation of the LN chip pairs prior to bonding

Due to the anisotropy of LN, bonding the upper and lower LN chip currently requires identical material orientation. Failing to do so will cause residual stress and possibly cracking during fabrication. It will also cause different SAW characteristics between the top and bottom surfaces of the nanoslit because of anisotropy. Therefore, bonding two LN chips with identical material orientation is highly recommended.

Alignment of the upper and lower chips

We visually perform the manual alignment and bonding. Introducing fiduciary markers and proper microscope-aided aligned bonding would surely improve device quality and yield.

O**ven heating temperature after initiating room-temperature bonding**

Heating at higher temperatures will help strengthen the bond. Heating to 300 °C for our LN bonding process produces at least 1 MPa bonding strength since it remains intact against comparable capillary and acoustic pressures in the nanoslit with SAW.

ACKNOWLEDGMENTS:

The authors are grateful to the University of California and the NANO3 facility at UC San Diego for provision of funds and facilities in support of this work. This work was performed in part at the San Diego Nanotechnology Infrastructure (SDNI) of UCSD, a member of the National Nanotechnology Coordinated Infrastructure, which is supported by the National Science Foundation (Grant ECCS–1542148). The work presented here was generously supported by a research grant from the W.M. Keck Foundation. The authors are also grateful for the support of this work by the Office of Naval Research (via Grant 12368098).

DISCLOSURES:

The authors have nothing to disclose.

REFERENCES:

1. Eijkel, J. C., & Van Den Berg, A. Nanofluidics: what is it and what can we expect from it? *Microfluidics and Nanofluidics*, **1**(3), 249-267 (2005).

2. Longhurst, M. J., & Quirke, N. Temperature-driven pumping of fluid through single-walled carbon nanotubes. *Nano Letters*, **7**(11), 3324-3328 (2007).

3. Wang, B., & Král, P. Coulombic dragging of molecules on surfaces induced by separately flowing liquids. *Journal of the American Chemical Society*, **128**(50), 15984-15985 (2006).

4. Insepov, Z., Wolf, D., & Hassanein, A. Nanopumping using carbon nanotubes. *Nano Letters*, **6**(9), 1893-1895 (2006).

5. Gong, X., et al. A charge-driven molecular water pump. *Nature Nanotechnology*, **2**(11), 709 (2007).
6. Joseph, S., & Aluru, N. R. Pumping of confined water in carbon nanotubes by rotation-translation coupling. *Physical Review Letters*, **101**(6), 064502 (2008).
7. Rinne, K. F., Gekle, S., Bonthuis, D. J., & Netz, R. R. Nanoscale pumping of water by AC electric fields. *Nano Letters*, **12**(4), 1780-1783 (2012).
8. Eslamian, M., & Saghir, M. Z. Novel thermophoretic particle separators: numerical analysis and simulation. *Applied Thermal Engineering*, **59**(1-2), 527-534 (2013).
9. Miansari, M., & Friend, J. R. Acoustic Nanofluidics via Room‐Temperature Lithium Niobate Bonding: A Platform for Actuation and Manipulation of Nanoconfined Fluids and Particles. *Advanced Functional Materials*, **26**(43), 7861-7872 (2016).
10. Minzioni, P., et al. Roadmap for optofluidics. *Journal of Optics*, **19**(9), 093003 (2017).
11. Connacher, W., et al. Micro/nano acoustofluidics: materials, phenomena, design, devices, and applications. *Lab on a Chip*, **18**(14), 1952-1996 (2018).
12. Ren, Z., et al. Etching characteristics of LiNbO3 in reactive ion etching and inductively coupled plasma. *Journal of Applied Physics*, **103**(3), 034109 (2008).
13. Winnall, S., & Winderbaum, S. Lithium niobate reactive ion etching. *Defence Science and Technology Organization Salisbury (Australia)*, No. DSTO-TN-0291 (2000).
14. Hu, H., Ricken, R., & Sohler, W. Etching of lithium niobate: micro-and nanometer structures for integrated optics. *Topical Meeting Photorefractive Materials, Effects, and Devices–Control of Light and Matter, Bad Honnef* (2009).
15. Jackel, J. L., Howard, R. E., Hu, E. L., & Lyman, S. P. Reactive ion etching of LiNbO3. *Applied Physics Letters*, **38**(11), 907-909 (1981).
16. Smith, S. E. Investigation of nanoscale etching and poling of lithium niobate (Doctoral dissertation, Montana State University-Bozeman, College of Engineering) (2014).
17. Tomita, Y., Sugimoto, M., & Eda, K. Direct bonding of LiNbO3 single crystals for optical waveguides. *Applied Physics Letters*, **66**(12), 1484-1485 (1995).
18. Howlader, M. M. R., Suga, T., & Kim, M. J. Room temperature bonding of silicon and lithium niobate. *Applied Physics Letters*, **89**(3), 031914 (2006).
19. Chang, C. M., et al. A parametric study of ICP-RIE etching on a lithium niobate substrate. *10th IEEE International Conference on Nano/Micro Engineered and Molecular Systems,* 485-486 (2015).
20. Queste, S., et al. Deep reactive ion etching of quartz, lithium niobate and lead titanate. *JNTE (Journées Nationales sur les Technologies) Proceedings* (2008).
21. Xu, J., Wang, C., Tian, Y., Wu, B., Wang, S., & Zhang, H. Glass-on-LiNbO3 heterostructure formed via a two-step plasma activated low-temperature direct bonding method. *Applied Surface Science*, **459**, 621-629 (2018).
22. Tulli, D., Janner, D., & Pruneri, V. Room temperature direct bonding of LiNbO3 crystal layers and its application to high-voltage optical sensing. *Journal of Micromechanics and Microengineering*, **21**(8), 085025 (2011).
23. Sridhar, M., Maurya, D.K., Friend, J.R., & Yeo, L.Y. Focused ion beam milling of microchannels in lithium niobate. *Biomicrofluidics*, **6**(012819) 2012.
24. Shilton, R.J., Yeo, L.Y., Friend, J.R. Drilling inlet and outlet ports in brittle substrates. *Chips and Tips. http://blogs.rsc.org/chipsandtips/2011/10/10/drilling-inlet-and-outlet-ports-in-brittle-ubstrates/?doing_wp_cron=1563672390.4860339164733886718750* (2011).

Figure 1

Click here to access/download;Figure;Figure 1 tiff.tiff

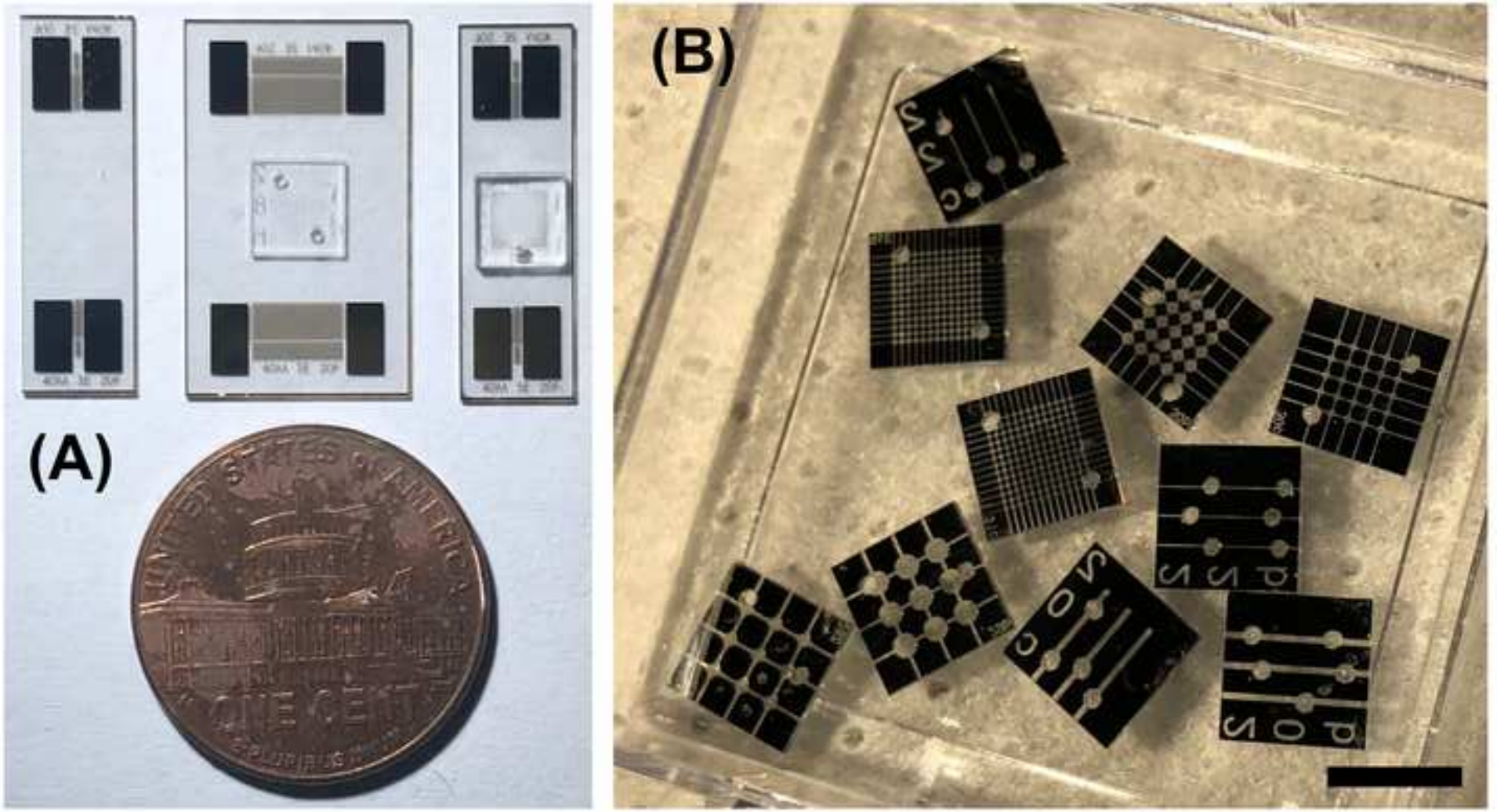

Figure 2

Click here to access/download;Figure;Figure 2 tiff.tiff

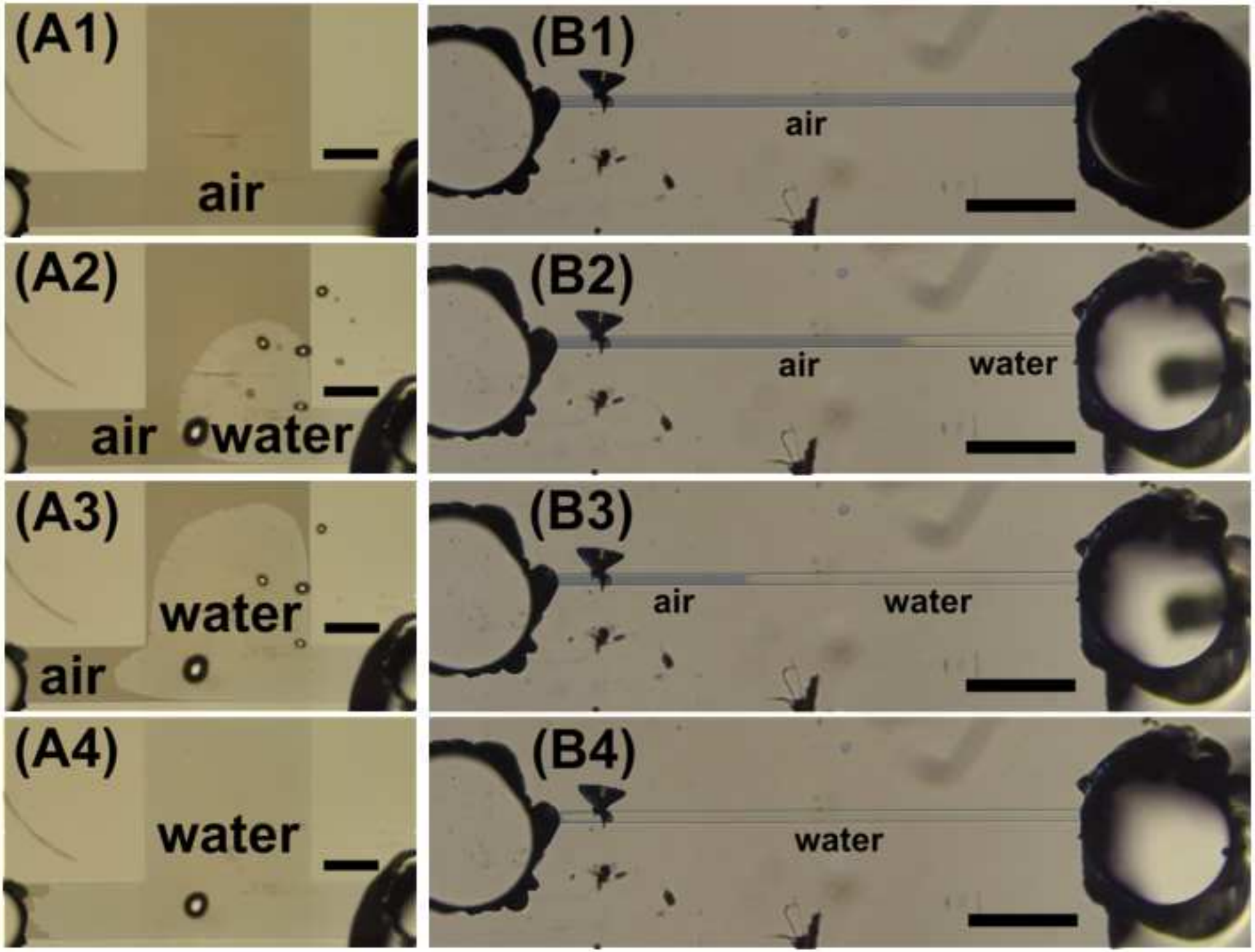

Figure 3

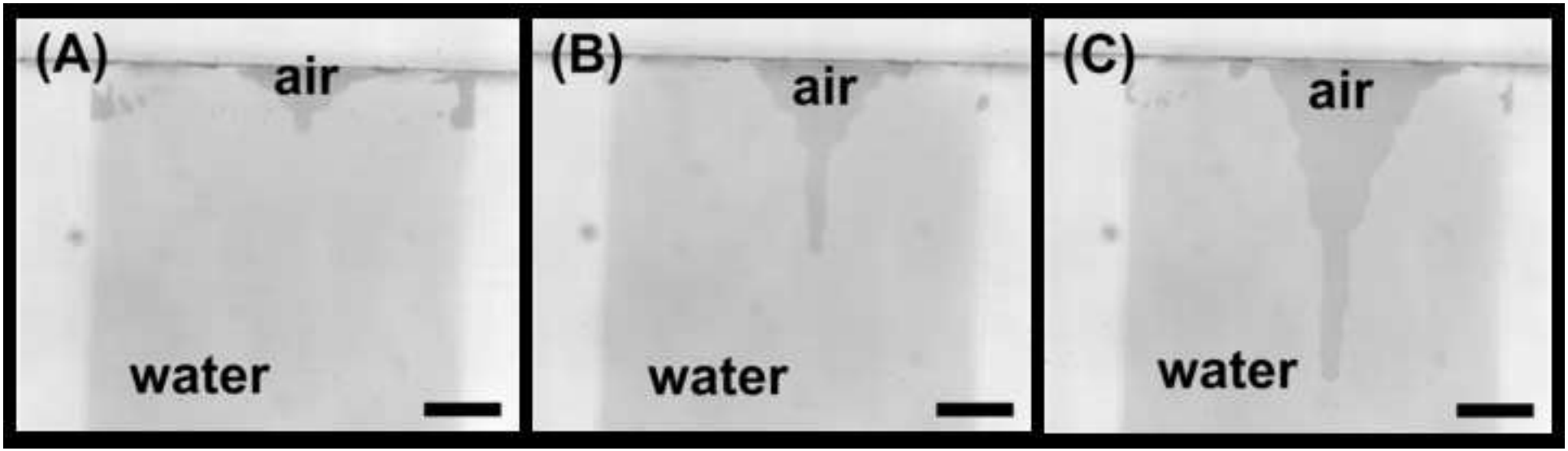

Figure 4

Click here to access/download;Figure;Figure 4 tiff.tiff

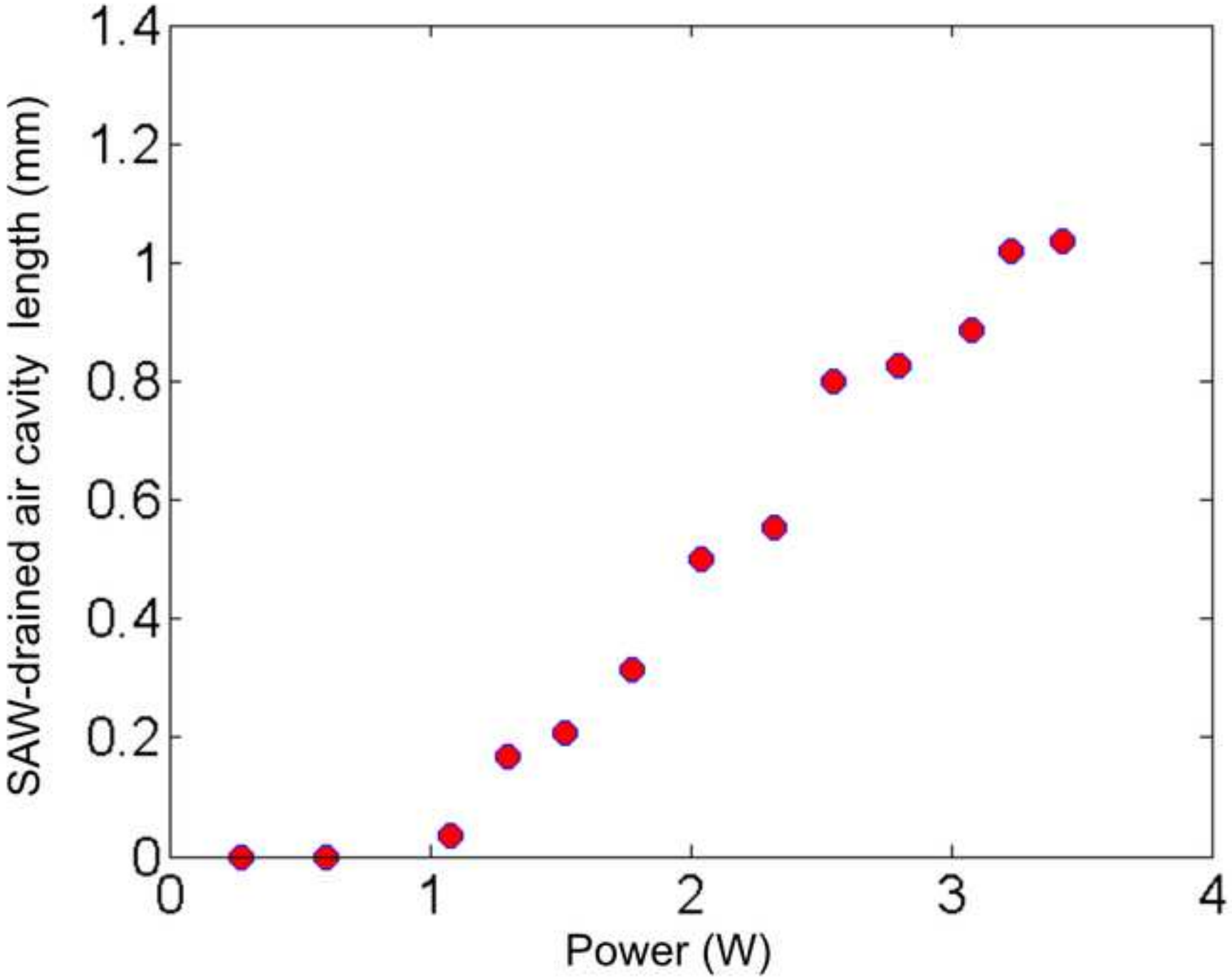

Name of Material/ Equipment	Company
Absorber	Dragon Skin, Smooth-On, Inc., Macungie, PA, USA
Amplifier	Mini-Circuits, Brooklyn, NY, USA
Camera	Nikon, Minato, Tokyo, Japan
Developer	Futurrex, NJ, USA
Diamond tip engraving pen	Malco, Memphis, TN, USA
Dicing saw	Disco, Tokyo, Japan
Heating oven	Carbolite, Hope Valley, UK
Hole driller	Dremel,Mount Prospect, Illinois
Inverted microscope	Amscope, Irvine, CA, USA
Lithium niobate substrate	PMOptics,Burlington, MA, USA
Mask aligner	Heidelberg Instruments, Heidelberg, Germany
Nano3 cleanroom facility	UCSD, La Jolla, CA, USA
Negative photoresist	Futurrex, NJ, USA
Oscilloscope	Keysight Technologies, Santa Rosa, CA, USA
Plasma surface activation	PVA TePla, Corona, CA, USA
Polarizer sheet	Edmund Optics, Barrington, NJ, USA
RIE etcher	Oxford Instruments, Abingdon, UK
Signal generator	NF Corporation, Yokohama, Japan
Sputter deposition	Denton Vacuum, NJ, USA
Teflon wafer dipper	ShapeMaster, Ogden, IL, USA

Catalog Number	Comments/Description
Dragon Skin 10 MEDIUM	
ZHL–1–2W–S+	
D5300	
RD6	
Malco A50 USA Made Carbide Tipped Scribe	
Disco Automatic Dicing Saw 3220	
HTCR 6/28	High Temperature Clean Room Oven - HTCR
Model #4000	4000 High Performance Variable Speed Rotary
IN480TC-FL-MF603	
PWLN-431232	4” double-side polished 0.5 mm thick 128°Y-rotated cut lithium niobate
MLA150	
	Fabrication process is performed in it.
NR9-1500PY	
InfiniiVision 2000 X-Series	
PS100	Tepla Asher
#86-182	
Plasmalab 100	
WF1967 multifunction generator	
Denton 18	Denton Discovery 18 Sputter System
SM4WD1	Wafer Dipper 4"

Editorial Comments:

1. Please take this opportunity to thoroughly proofread the manuscript to ensure that there are no spelling or grammar issues.

Our response: We have thoroughly proofread the manuscript and fixed the spelling and grammar issues, with a large number of changes large and small to try to make the manuscript appropriate for publication. Most notably, and as discussed with the editor, we have culled the SAW electrode and device fabrication part from this manuscript in order to focus on the nanoslit content.

2. Please revise the Discussion to explicitly cover the following in detail in 3-6 paragraphs with citations:
a) Critical steps within the protocol
b) Any modifications and troubleshooting of the technique
c) Any limitations of the technique
d) The significance with respect to existing methods
e) Any future applications of the technique

Our response: The Discussion has been revised into 6 paragraphs with citations.

3. Step 2.1: To film step 2.1, steps 1.1-1.6 need to be highlighted as well.

Our response: Step 2.1 has been dehighlighted. Step 1.1-1.6 can be announced as “normal photolithography procedure” due to the page and video limit.

4. Please avoid long steps/notes (more than 4 lines).

Our response: fixed for the most part. There are few steps that require careful explanation that pushes the length beyond the 4-line limit, but we have acted to cut the text content wherever possible.

5. Please do not use more than 1 note for each step.

Our response: We have changed to use no more than 1 note for each step.

Under Protocol section, beginning in line 101 originally read:
“NOTE: Because of the *pyroelectric* property of LN, it will generate static charge and associated stress within the wafer during heating and cooling. If the temperature of the LN wafer is suddenly changed, for example by directly transferring the LN wafer onto or off of the hotplate at 150 °C, the sudden temperature change will cause thermal shock within the wafer, likely shattering it. The presence of nonuniform metal on the surface, such as electrodes, significantly enhances the risk of wafer shattering due to differential stress. In applications where temperature excursions are necessary during fabrication or use, and

the transparency of the LN is not important, consider using so-called “black” LN or more accurately *reduced* LN, which is a dark brown translucent color but more importantly has negligible pyroelectricity.

NOTE: The temperature ramp rate is around 10 °C/min when heating and -3 °C/min when cooling.”

Under Protocol section, beginning in line 101 now reads:
“NOTE: Because of the *pyroelectric* property of LN, it will generate static charge and associated stress within the wafer during heating and cooling. If the temperature of the LN wafer is suddenly changed, for example by directly transferring the LN wafer onto or off of the hotplate at 150 °C, the sudden temperature change will cause thermal shock within the wafer, likely shattering it. Specifically, the temperature ramp rate is around 10 °C/min when heating and -3 °C/min when cooling. The presence of nonuniform metal on the surface, such as electrodes, significantly enhances the risk of wafer shattering due to differential stress. In applications where temperature excursions are necessary during fabrication or use, and the transparency of the LN is not important, consider using so-called “black” LN or more accurately *reduced* LN, which is a dark brown translucent color but more importantly has negligible pyroelectricity.”

Under Protocol section, beginning in line 162 originally read:
“NOTE: The protocol can be paused here.

NOTE: Instead of a saw, a diamond-tipped wafer scribe (or even a glass cutter) can be used to dice the LN wafer with some practice, though due to the anisotropy of LN it is important to scribe and break the wafer *first* along scribe lines *perpendicular to the X-axis*, followed by those lines along the X-axis.”

Under Protocol section, beginning in line 161 now reads:
“NOTE: Instead of a saw, a diamond-tipped wafer scribe (or even a glass cutter) can be used to dice the LN wafer with some practice, though due to the anisotropy of LN it is important to scribe and break the wafer *first* along scribe lines *perpendicular to the X-axis*, followed by those lines along the X-axis. The protocol can be paused here.”

Under Protocol section, beginning in line 226 originally read:
“NOTE: It is exceedingly difficult to distinguish which side of the LN chip actually contains the etched nanoscale depression after the Cr is removed.

NOTE: Sonication time will depend upon the etching rate and the Cr mask thickness.

NOTE: The protocol can be paused here.”

Under Protocol section, beginning in line 223 now reads:
“NOTE: It is exceedingly difficult to distinguish which side of the LN chip actually contains

the etched nanoscale depression after the Cr is removed. Sonication time will depend upon the etching rate and the Cr mask thickness. The protocol can be paused here."

Under Protocol section, beginning in line 253 originally read:
"NOTE: By rinsing the LN chips only once with a single DI water bath, residue may remain on the LN chip surfaces and ruin the bonding.

NOTE: Gold electrodes are used for IDTs because of their good resistance to piranha solution."

Under Protocol section, beginning in line 223 now reads:
"NOTE: By rinsing the LN chips only once with a single DI water bath, residue may remain on the LN chip surfaces and ruin the bonding. Gold electrodes are used for IDTs because of their good resistance to piranha solution."

Under Protocol section, beginning in line 278 originally read:
"NOTE: Because the bonding between hydroxyl groups will produce water molecules, high-temperature heating after bonding is used to dehydrate the bonding interface of the two LN chips to dramatically increase the bond strength.

NOTE: Hand-tight or spring-clamp clamping is sufficient.

NOTE: Attempting to bond two chips of different orientations or materials may cause cracks during heating and cooling due to mismatched thermal expansion and consequent stress.

NOTE: The protocol can be paused here."

Under Protocol section, beginning in line 271 now reads:
"NOTE: Because the bonding between hydroxyl groups will produce water molecules, high-temperature heating after bonding is used to dehydrate the bonding interface of the two LN chips to dramatically increase the bond strength. Hand-tight or spring-clamp clamping is sufficient. Attempting to bond two chips of different orientations or materials may cause cracks during heating and cooling due to mismatched thermal expansion and consequent stress. The protocol can be paused here."

Under Protocol section, beginning in line 297 originally read:
"NOTE: Any dust or debris will block the inlets or outlets when the liquid evaporates. So ultrapure liquid is highly recommended to prevent clogging of the nanoscale channel.

NOTE: Most light is at least partially circularly polarized. Objects illuminated with this light and seen through LN will appear twice in slightly different locations due to the different indices of refraction along the X and Y axes of the LN. By using a linear polarizing filter aligned to either the X or Y axis of the LN, light for one of the images will be blocked, leaving a single image to view during observations. More light is necessary in many cases

to overcome the light loss with the polarizing filter."

Under Protocol section, beginning in line 286 now reads:
"NOTE: Most light is at least partially circularly polarized. Objects illuminated with this light and seen through LN will appear twice in slightly different locations due to the different indices of refraction along the X and Y axes of the LN. By using a linear polarizing filter aligned to either the X or Y axis of the LN, light for one of the images will be blocked, leaving a single image to view during observations. More light is necessary in many cases to overcome the light loss with the polarizing filter. Additionally, any dust or debris will block the inlets or outlets when the liquid evaporates. So ultrapure liquid is highly recommended to prevent clogging of the nanoscale channel."

6. For in-text referencing, the superscripted reference number should be inserted before a comma or period.

Our response: The superscripted reference numbers have been changed to be inserted before a comma or period, as shown in the revised manuscript.

7. After you make all changes, please ensure that the highlighted protocol steps are fewer than 2.75 pages.

Our response: After all the changes, the highlighted protocol steps are fewer than 2.75 pages.